Check for updates



American Society of Hematology 2021 L Street NW, Suite 900, Washington, DC 20036 Phone: 202-776-0544 | Fax 202-776-0545

Post-transcriptional depletion of ribosome biogenesis factors engenders therapeutic vulnerabilities in NPM1-mutant AML

Tracking no: BLD-2024-026113R2

Aristi Damaskou (University of Cambridge, United Kingdom) Rachael Wilson (University of Cambridge, United Kingdom) Malgorzata Gozdecka (University of Cambridge, United Kingdom) George Giotopoulos (University of Cambridge, United Kingdom) Ryan Asby (University of Cambridge, United Kingdom) Maria Eleftheriou (University of Cambridge, United Kingdom) Muxin Gu (University of Cambridge, United Kingdom) Christian Récher (CHU de Toulouse, France) Véronique Mansat- De Mas (CHU Toulouse, IUCTO, France) Francois Vergez (IUCT, France) Ambrine Sahal (Centre de Recherches en Cancérologie de Toulouse, Université de Toulouse, France) Binje Vick (Helmholtz Munich, Germany) Evangelia Papachristou (University of Cambridge, United Kingdom) Ashley Sawle (University of Cambridge, United Kingdom) Eliza Yankova (University of Cambridge, United Kingdom) Monika Dudek (University of Cambridge, United Kingdom) Xiaoxuan Liu (University of Cambridge, United Kingdom) James Russell (University of Cambridge, United Kingdom) Justyna Rak (Lund University, Sweden) Christine Hilcenko (University of Cambridge, United Kingdom) Clive D'Santos (University of Cambridge, United Kingdom) Irmela Jeremias (Helmholtz Zentrum München, Germany) Jean-Emmanuel Sarry (INSERM, France) Konstantinos Tzelepis (University of Cambridge, United Kingdom) Brian Huntly (University of Cambridge, United Kingdom) Alan Warren (University of Cambridge, United Kingdom) Omid Tavana (Astrazeneca, United States) George Vassiliou (University of Cambridge, United Kingdom)

Abstract:

NPM1 is a multifunctional phosphoprotein with key roles in ribosome biogenesis amongst its many functions. NPM1 gene mutations drive 30% of acute myeloid leukemia (AML) cases. The mutations disrupt a nucleolar localization signal (NoLS) and create a novel nuclear export signal (NES), leading to cytoplasmic displacement of the protein (NPM1c). NPM1c mutations prime hematopoietic progenitors to leukemic transformation, but their precise molecular consequences remain elusive. Here, we first examine the effects of isolated NPM1c mutations on the global proteome of preleukemic hematopoietic stem and progenitor cells (HSPCs) using conditional knock-in Npm1cA/+ mice. We discover that many proteins involved in ribosome biogenesis are significantly depleted in these murine HSPCs, but also importantly in human NPM1-mutant AMLs. In line with this, we found that preleukemic Npm1cA/+ HSPCs display higher sensitivity to RNA polymerase I inhibitors, including Actinomycin D (ActD), compared to Npm1+/+ cells. Combination treatment with ActD and Venetoclax inhibited the growth and colony forming ability of pre-leukemic and leukemic NPM1c+ cells, whilst low-dose ActD treatment was able to re-sensitize resistant NPM1c+ cells to Venetoclax. Furthermore, using data from CRISPR dropout screens, we identified and validated TSR3, a 40S ribosomal maturation factor whose knock-out preferentially inhibited the proliferation of NPM1c+ AML cells by activating a p53-dependent apoptotic response. Similarly to low-dose ActD treatment, TSR3 depletion could partially restore sensitivity to Venetoclax in therapy-resistant NPM1c+ AML models. Our findings propose that targeted disruption of ribosome biogenesis should be explored as a therapeutic strategy against NPM1-mutant AML.

Conflict of interest: COI declared - see note

COI notes: G.S.V. is a consultant to STRM.BIO and holds a research grant from AstraZeneca (G113590) that funded part of the research presented here. K.T. is a shareholder of and has received research funding from Storm Therapeutics Ltd. O.T is an AstraZeneca employee and shareholder. All other authors declare no competing financial interests.

Preprint server: No;

Author contributions and disclosures: G.S.V. conceived and supervised the study. G.S.V. and A.D. designed the experimental plan. A.D. carried out the majority of experiments with help from R.W. M.G. contributed to experimental design and provided scientific expertise. The in vivo PDX experiment was performed with help from G.G. (study design, animal procedures, imaging), R.A. (animal procedures, animal collection) and G.S.V. (intravenous injections). M.E. contributed to immunofluorescence imaging and animal collection and processing. M.Gu performed bioinformatic analysis and data deposition for the RNA-seq experiments. Primary AML characterization, sample collection and PDX generation were carried out by C.R. (clinician), V.D.M. (biobanking), F.V. (diagnosis), A.S. (PDX generation), B.V. (passaging and introduction of luciferase reporter) and I.J. and J.E.S. (supervision). E.K.P., A.S. and C.D.S. performed, analyzed and provided scientific expertise for the pre-leukemic TMT proteomics experiment. E.Y., M.D., X.L., J.R and J.R. contributed to animal collection and processing. C.H. performed polysome profiling. I.J., J.E.S, K.T, B.J.P.H, A.J.W and O.T. provided scientific expertise. G.S.V. and A.D. prepared the manuscript with help from all authors.

Non-author contributions and disclosures: No;

Agreement to Share Publication-Related Data and Data Sharing Statement: The mass spectrometry proteomics data have been deposited to the ProteomeXchange Consortium via the PRIDE13 partner repository with the dataset identifier PXD053249 (token: 57CDevKiMF0e). RNA-seq raw data have been deposited in Gene Expression Omnibus with the accession numbers GSE264084 (human, token:apgbuwoqvbyrpcf) and GSE264322 (mouse, token: sbohcqiyblyjncz).

Clinical trial registration information (if any):

Proteomic Insights Into NPM1-Mutant Pre-Leukemia and Acute Myeloid Leukemia (AML)

Context of Research

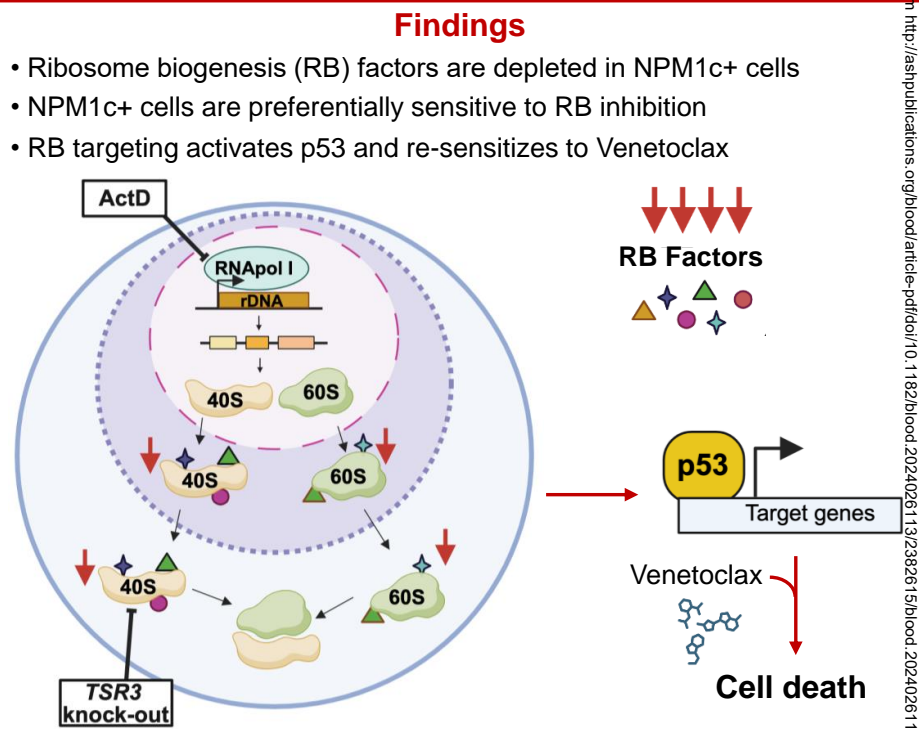
NPM1 mutations (NPM1c) prime hematopoietic progenitors for AML transformation.

The consequences of *NPM1c* mutations at the proteomic level remain largely unexplored

Methods Mass Spectrometry NPM1c+ Npm1cA/+ AML pre-AML (Kramer et al. (this study) Blood 2022) **Target Identification & Validation**

Findings

- Ribosome biogenesis (RB) factors are depleted in NPM1c+ cells
- NPM1c+ cells are preferentially sensitive to RB inhibition
- RB targeting activates p53 and re-sensitizes to Venetoclax



blood

Visual Abstract

Conclusions: Pre-leukemic and leukemic NPM1-mutant cells have reduced levels of several ribosome biogenesis proteins. Targeted inhibition of ribosome biogenesis with Actinomycin D or TSR3 disruption is a potential therapeutic strategy against NPM1mutant AML.

Damaskou et al. DOI: 10.xxxx/blood.2025xxxxxxx

1 Post-transcriptional depletion of ribosome biogenesis factors engenders therapeutic 2 vulnerabilities in NPM1-mutant AML

3

- Aristi Damaskou^{1,2*}, Rachael Wilson^{1,2}, Malgorzata Gozdecka^{1,2}, George Giotopoulos^{1,2}, Ryan 4
- Asby^{1,2}, Maria Eleftheriou^{1,2,3}, Muxin Gu^{1,2}, Christian Récher^{4,5,6,7}, Véronique De Mas^{4,5,6,7}, 5
- Francois Vergez^{4,5,6,7}, Ambrine Sahal^{4,5,6}, Binje Vick^{8,9}, Evangelia K. Papachristou¹⁰, Ashley 6
- Sawle¹⁰, Eliza Yankova^{1,2,3}, Monika Dudek^{1,2}, Xiaoxuan Liu^{1,2}, James Russell^{1,2}, Justyna Rak^{1,2}, Christine Hilcenko^{1,2,11,12}, Clive D' Santos¹⁰, Irmela Jeremias^{8,9,13}, Jean-Emmanuel Sarry^{4,5,6}, 7
- 8
- Konstantinos Tzelepis^{1,2,3}, Brian J. P. Huntly^{1,2,11}, Alan J. Warren^{1,2,11}, Omid Tavana¹⁴, George 9
- S. Vassiliou^{1,2,15*}. 10

11

- 12 1. Cambridge Stem Cell Institute, University of Cambridge, Cambridge, United Kingdom.
- 2. Department of Haematology, University of Cambridge, Cambridge, United Kingdom. 13
- 14 3. Milner Therapeutics Institute, University of Cambridge, Puddicombe Way, Cambridge,
- 15 United Kingdom.
- 16 4. Centre de Recherches en Cancérologie de Toulouse, Université de Toulouse, Inserm
- 17 U1037, CNRS U5077, Toulouse, France.
- 18 5. LabEx Toucan, Toulouse, France.
- 19 6. Équipe Labellisée Ligue Nationale Contre le Cancer 2023, Toulouse, France.
- 20 7. Centre Hospitalier Universitaire de Toulouse, Institut Universitaire du Cancer de Toulouse
- 21 Oncopole, Service d'Hématologie, Toulouse, France
- 8. Research Unit Apoptosis in Hematopoietic Stem Cells, Helmholtz Zentrum München, 22
- 23 German Research Center for Environmental Health (HMGU), Munich, Germany.
- 24 9. German Cancer Consortium (DKTK), Partner Site Munich, Munich, Germany.
- 25 10. Cancer Research UK Cambridge Institute, University of Cambridge, Li Ka Shing Centre,
- 26 Cambridge, United Kingdom.
- 27 11. Cambridge Institute for Medical Research, University of Cambridge, Cambridge, United
- 28 Kingdom.
- 29 12. Department of Infectious Disease, Imperial College London, London, United Kingdom.
- 30 13. Department of Pediatrics, Dr. von Hauner Children's Hospital, University Hospital, LMU,
- 31 Munich, Germany.
- 32 14. Haematology R&D, AstraZeneca, Waltham, Massachusetts, United States of America.
- 33 15. Department of Haematology, Cambridge University Hospitals NHS Trust, Cambridge,
- 34 United Kingdom.
- 35 *Correspondence: George S Vassiliou (gsv20@cam.ac.uk), Aristi Damaskou
- 36 (ad971@cam.ac.uk)

37

- 38 Short title: Targeting ribosome biogenesis in NPM1-mutant AML
- 39 Word Count (Abstract): 243
- 40 Word Count (Text): 3,970 (Introduction, Methods, Results, Discussion)
- 41 Figure Count: 7
- 42 Reference Count: 56
- 43 Appropriate Scientific Category: Myeloid Neoplasia

Data sharing

RNA-seq data have been deposited to Gene Expression Omnibus (accession numbers GSE264084 and GSE264322). Mass spectrometry proteomics data have been deposited to the ProteomeXchange Consortium (dataset identifier PXD053249). Data are available on request from the corresponding authors George S Vassiliou (gsv20@cam.ac.uk) and Aristi Damaskou (ad971@cam.ac.uk).

51 52

53

54

55

56

45

46

47

48

49

50

Key points

- Pre-leukemic and leukemic *NPM1*-mutant cells have reduced levels of several ribosome biogenesis proteins
- Targeted therapeutic disruption of ribosome biogenesis is a potential strategy against *NPM1*-mutant acute myeloid leukemia

57

58

59

60

61

62

63

64

65

66

67

68

69

70

71

72

73

74

75

76

Abstract

NPM1 is a multifunctional phosphoprotein with key roles in ribosome biogenesis amongst its many functions. NPM1 gene mutations drive 30% of acute myeloid leukemia (AML) cases. The mutations disrupt a nucleolar localization signal (NoLS) and create a novel nuclear export signal (NES), leading to cytoplasmic displacement of the protein (NPM1c). NPM1c mutations prime hematopoietic progenitors to leukemic transformation, but their precise molecular consequences remain elusive. Here, we first examine the effects of isolated NPM1c mutations on the global proteome of preleukemic hematopoietic stem and progenitor cells (HSPCs) using conditional knock-in Npm1^{cA/+} mice. We discover that many proteins involved in ribosome biogenesis are significantly depleted in these murine HSPCs, but also importantly in human NPM1mutant AMLs. In line with this, we found that pre-leukemic Npm1^{cA/+} HSPCs display higher sensitivity to RNA polymerase I inhibitors, including Actinomycin D (ActD), compared to Npm1^{+/+} cells. Combination treatment with ActD and Venetoclax inhibited the growth and colony forming ability of pre-leukemic and leukemic NPM1c+ cells, whilst low-dose ActD treatment was able to re-sensitize resistant NPM1c+ cells to Venetoclax. Furthermore, using data from CRISPR dropout screens, we identified and validated TSR3, a 40S ribosomal maturation factor whose knock-out preferentially inhibited the proliferation of NPM1c+ AML cells by activating a p53dependent apoptotic response. Similarly to low-dose ActD treatment, *TSR3* depletion could partially restore sensitivity to Venetoclax in therapy-resistant NPM1c+ AML models. Our findings propose that targeted disruption of ribosome biogenesis should be explored as a therapeutic strategy against *NPM1*-mutant AML.

Introduction

Nucleophosmin, coded by the *NPM1* gene, is a highly abundant phosphoprotein involved in diverse cellular processes^{1–6}. It can shuttle between the nucleus and cytoplasm, but at steady state is primarily located at the nucleolus, the main site of ribosomal RNA (rRNA) transcription and early ribosome biogenesis⁷. More specifically, Nucleophosmin is located at the outer, granular component (GC) of the nucleolus⁸, contributes to maintaining the organelle's structure^{9,10} and is involved in rRNA 2'-O-methylation¹¹.

Somatic mutations affecting the *NPM1* gene are found in ~30% of cases of acute myeloid leukemia (AML)^{12,13} and define the most common AML subtype. AML-associated *NPM1* mutations, usually 4-basepair duplications/insertions within the gene's final exon, disrupt a nucleolar localization signal (NoLS) and create a novel nuclear export signal (NES). As a result, mutant Nucleophosmin is aberrantly localized to the cytoplasm (NPM1c) through interaction with XPO1, a major effector of nucleocytoplasmic traffic¹⁴. The current standard of care treatment for patients with *NPM1c*-mutant AML is 3+7 chemotherapy, while for patients carrying *FLT3* co-mutations, such as internal tandem duplications (ITDs), a FLT3 inhibitor is incorporated into first-line treatment^{15,16}. Most patients enter complete remission, but approximately half relapse and most of them succumb to their disease, highlighting the need for new therapies¹⁷.

Despite its high prevalence in AML, the molecular consequences of the *NPM1c* mutation are incompletely understood, which poses an obstacle to the design of effective therapeutic strategies¹⁸. Recent advances have given insights into the transcriptomic and epigenetic

effects of *NPM1c* mutations¹⁹, but less is known about its global post-transcriptional and proteomic consequences.

In this study, we determine the global proteomic consequences of isolated *NPM1c* mutations in pre-leukemic hematopoietic progenitors from knock-in *Npm1c*-mutant mice, which faithfully recapitulate the human mutations^{19–21}. We then investigate which changes are also detected in full blown *NPM1*-mutant AML²² and examine these against CRISPR knock-out screens^{23–25} to identify potential therapeutic targets. Notably, we find significant decreases in abundance of multiple ribosome biogenesis factors in NPM1c+ pre-leukemia that are also observed in human NPM1c+ AML and are associated with increased sensitivity to the RNA polymerase (pol) I inhibitor Actinomycin D (ActD) alone and particularly in combination with the Bcl-2 inhibitor Venetoclax. Focusing on individual targets, we discover that *NPM1c*-mutant cells are dependent on *TSR3*, a normally non-essential maturation factor of the 40S ribosomal subunit. Finally, we show that both low-dose ActD treatment and *TSR3* knock-out induce resensitization to Venetoclax in previously resistant NPM1c+ leukemia cells.

Methods (also see Supplementary Methods)

Mouse model

Mx1-Cre; Npm1 mice have been described previously 19,20. Cre expression was induced in 8-10 weeks old *Mx1-Cre; Npm1* mice by administration of plpC (Cat# P1530, Sigma-Aldrich). Blood counts were calculated by a Scil Vet abc hematology analyzer. All mice were kept in a pathogen-free environment and all procedures were performed according to the regulation of the UK Home office, under project licence PP3797858, in accordance with the Animal Scientific Procedures Act 1986.

Proteomic analysis of pre-leukemic murine hematopoietic progenitors

7 Npm1^{cA/+} and 5 control Npm1^{+/+} mice were collected 8 weeks post-plpC and the bone marrow lin- cells were subjected to proteomic analysis (Supplementary Table S1). Sample preparation, MS analysis and data processing are described in detail in Supplementary Methods.

Proteomic and RNA expression analysis of AML patient samples

Experimental procedures and datasets can be found in Kramer et al²². t-test was used to calculate p values for differences between the NPM1wt and NPM1c+ AML groups, followed by multiple hypothesis correction using the Benjamini-Hochberg method.

Study of patient-derived NPM1-mutant AML cells

For patient-derived xenograft (PDX) studies, 1x10⁶ cells of a luciferase-expressing *NPM1*-mutant AML PDX were injected intravenously (IV) into NOD.Cg-Prkdcscid Il2rgtm1Wjl/SzJ (NSG) mice and animals were treated with intraperitoneal ActD or vehicle from day 35 after transplantation and monitored for AML tumor volume and survival. Detailed experimental procedures are provided in Supplementary Methods.

NPM1-mutant normal karyotype AML cells were obtained from a 33-year-old male with the patient's informed consent as part of the H2mopathies Inserm Midi-Pyr2n2es (HIMIP) collection (BB-0033-00060). According to the French law, the HIMIP collection has been declared to the Ministry of Higher Education and Research (DC 2008-307 collection 1) and obtained a transfer agreement (AC 2008-129) after approbation by the Comit2 de Protection des Personnes Sud-Ouest et Outremer II (ethical committee). The study was performed in accordance with the Declaration of Helsinki.

Results

Npm1^{cA/+} hematopoietic progenitors have reduced levels of ribosome biogenesis proteins

We collected bone marrow lineage depleted (lin-) hematopoietic stem/progenitor cells (HSPCs) 8 weeks after activation of the conditional *Npm1cA* allele in *Mx1-Cre; Npm1^{flox-cA/+}* mice²⁰. At that stage, the mice displayed normal hematological parameters and no signs of leukemia (Supplementary Figure S1A-S1D), but the characteristic *Npm1c*-associated *HoxA* and *HoxB* gene upregulation was clearly evident in HSPCs (Supplementary Figure S1E, Supplementary Table S2). In line with this, *Npm1^{cA/+}* HSPCs showed enhanced serial re-plating in colony-forming unit (CFU) assays, compared to their wild-type counterparts (Supplementary Figure S1F-S1G).

To capture the global impact of isolated Npm1c mutations at the protein level, we performed tandem mass tag (TMT)-based quantitative proteomics in HSPCs from Npm1^{cA/+} mutant (n=7) vs Npm1^{+/+} (n=5) mice (Figure 1A). Of 7,409 proteins detected overall, we found 58 highconfidence proteins whose abundance was significantly different (p_{adi} <0.05) between Npm1^{cA/+} and Npm1^{+/+} HSPCs (Figure 1B, Supplementary Table S3). Notably, NPM1 protein levels were found to be significantly reduced in Npm1^{cA/+} mice. However, examination of the identified peptide spectra, revealed that this was because the only NPM1-derived peptide detected was unique to the wild-type protein (amino acids 276-289). With no mutant-specific peptides identified, this resulted in an apparent reduction in NPM1 protein levels in heterozygous mice. The top three proteins with the most significantly increased levels were the polyol pathway enzyme SORD (Sorbitol Dehydrogenase), the centrosomal protein CEP44 (Centrosomal Protein 44), and the F13A1 (Coagulation Factor XIII A Chain) blood coagulation factor (Supplementary Figure S2A-S2C). In addition, among proteins showing increased abundance were several members of the Karyopherin (KPN) family (Supplementary Figure S2D), mirroring recent findings in human NPM1c-mutant AML²². Interestingly, NPM1c+ OCI-AML3 cells were shown to be particularly sensitive to KPNA2 knock-out (Dep Map^{24,25}, Supplementary Figure S2F-S2G).

Among the 31 proteins showing decreased abundance in *Npm1*^{cA/+} HSPCs, there were several ribosome-related proteins, including ribosome biogenesis factors and structural constituents of ribosomes⁷. Significantly depleted proteins included KRI1 (KRI1 Homolog)²⁶, RIOX1 (Ribosomal Oxygenase 1)²⁷, RRS1 (Ribosome Biogenesis Regulator 1 Homolog)^{28,29} and RPL22L1 (Ribosomal Protein L22 Like 1)³⁰ (Figure 1C-1F), none of which showed reduction at the mRNA level (Figure 1G). Gene ontology (GO) term analysis of all depleted proteins (n=270) amongst the top 500 differentially abundant proteins showed enrichment for the pre-ribosome, and biological processes involving ribosomal RNA (rRNA) processing and ribosome biogenesis (Supplementary Figure S3A, Supplementary Table S4). Polysome profiling of whole bone marrow cells from *Npm1*^{cA/+} and control *Npm1*^{+/+} mice showed no major differences, although there was a trend towards higher abundance for the 40S ribosomal subunit in the mutant cells (Supplementary Figure S3B-S3E).

Ribosome biogenesis factors are depleted in human NPM1c+ AML

To pinpoint which changes identified in NPM1c+ pre-leukemic cells can also be detected after progression to AML, we examined recently reported TMT proteomics data from bone marrow samples of 44 de novo AML patients, including 8 with NPM1c+ AML²². By comparing protein levels between NPM1c+ and NPM1 wild-type (NPM1wt) AMLs, we identified only 11 significantly differentially abundant proteins (p_{adj} <0.05), among which KRI1 was the most depleted (Figure 2A-2B, Supplementary Table S5). Importantly, GO analysis of all depleted proteins (n=191) amongst the top 500 differentially abundant proteins revealed an enrichment for ribosome biogenesis factors, rRNA processing enzymes and maturation factors of rRNA precursors (Supplementary Figure S4A, Supplementary Table S6), similar to the murine pre-leukemic cells. RIOX1, RRS1 and RPL22L1, all of which were significantly depleted in pre-leukemic Npm1^{cA/+} cells, also showed reduced abundance in NPM1c+ AML (Figure 2C-2E), albeit without reaching significance after correcting for multiple testing. Other ribosome-related proteins that were depleted in NPM1c+ AML included KRR1 (KRR1 Small Subunit Processome Component Homolog), an important interactor of KRI1³¹, RPS9 (Ribosomal Protein S9) and RBIS (Ribosomal Biogenesis Factor) (Supplementary Figure S4B-S4D). Notably, none of the above candidates showed downregulation in RNA-seq data from the same patients, suggesting that these genes/proteins are regulated post-transcriptionally (Figure 2F-2I, Supplementary Figure S4E-S4G). Finally, no significant differences were observed in the abundance of the above proteins between NPM1c+; FLT3-ITD+ and all other NPM1c+ AMLs (Supplementary Figure S4H), suggesting that these changes were not related to FLT3-ITD, the most common co-mutation of NPM1c in AML.

220

221

222

223

224

225

226

227

228

198

199

200

201

202

203

204

205

206

207

208

209

210

211

212

213

214

215

216

217

218

219

Pre-leukemic Npm1^{cA/+} HSPCs show enhanced sensitivity to RNA pol I inhibitors

In light of the mis-localization of mutant and the reduced levels of wild-type NPM1, targeting ribosome homeostasis has been previously proposed as a therapeutic strategy against *NPM1*-mutant AML $^{32-34}$. Our data suggest that, in addition to the reduced levels of wild-type NPM1 in the nucleolus, mutant cells are also depleted of several ribosome biogenesis factors. We hypothesized that this depletion creates a vulnerability that can be therapeutically exploited to specifically target mutant cells. To test this, we compared the responses of pre-leukemic $Npm1^{cA/+}$ vs control $Npm1^{t/+}$ HSPCs to drugs that modulate ribosome biogenesis, including

Actinomycin D (ActD) and other RNA pol I inhibitors. Indeed, we found that compared to $Npm1^{t/+}$ cells, pre-leukemic $Npm1^{cA/+}$ lin- cells were significantly more sensitive to ActD treatment (Figure 3A-3C), particularly at lower concentrations where the drug effects are known to be on-target (Supplementary Figure S5A)³⁵. Following treatment with low-dose ActD (1 nM), both mutant and wild-type HSPCs exhibited characteristic features of nucleolar stress, including a shift in nucleolar shape from irregular to round conformation (Figure 3D)^{36,37}. This suggests that both cell types activate a nucleolar stress response, although impact on survival is greater for NPM1c+ cells. Nucleoplasmic dislocation of wild-type NPM1, another indicator of nucleolar stress^{34,37,38}, was observed in pre-leukemic $Npm1^{cA/+}$ lin- cells treated with higher drug doses (5 nM) (Supplementary Figure S5B). No DNA damage was observed in $Npm1^{cA/+}$ lin- cells following treatment with 2.5 nM ActD for 48 hours (Supplementary Figure S5C).

To further test if the preferential sensitivity of $Npm1^{cA/+}$ cells to ActD was due to RNA Pol I inhibition, and not due to off-target effects, we then tested BMH-21 and CX-5461, two more recently developed small-molecule inhibitors with different modes of RNA pol I inhibition^{39–41}. Similarly to ActD, we found that $Npm1^{cA/+}$ HSPCs were significantly more sensitive to both agents compared to wild-type $Npm1^{+/+}$ cells (Figure 3E-3F, Supplementary Figure S5D- S5G). While off-target effects cannot be entirely excluded, the consistent phenotype observed across the three chemically distinct compounds, suggests that Npm1c-specificity is primarily driven by on-target RNA pol I inhibition. By contrast, we did not observe differential sensitivity between $Npm1^{cA/+}$ and $Npm1^{+/+}$ HSPCs to cycloheximide, a drug that inhibits translational elongation (Figure 3G).

Single-agent ActD inhibits expansion of an NPM1-mutant AML patient-derived xenograft (PDX)

To investigate the effects of ActD treatment *in vivo* using a clinically relevant AML model, we used a luciferase-expressing *NPM1*-mutant PDX harboring *DNMT3A R882H*, *FLT3-ITD* and *RAD21 R146G* co-mutations. One million NPM1c+ AML PDX cells were injected intravenously (IV) into 12 NSG mice (Figure 4A, Supplementary Figure S6A). After 35 days mice were allocated into two groups of similar AML burden (Figure 4B) to receive ActD (0.1 mg kg⁻¹) or vehicle twice weekly for 5 weeks. Repeat bioluminescent imaging revealed a significant reduction of AML burden in ActD-treated animals at 45 and 58 days post IV injection (Figure

4C-4E). Dosing was reduced to 0.06 mg kg⁻¹ once weekly for another 3 weeks and animals were monitored until they developed leukemia symptoms. ActD-treated animals had a significantly longer survival at 90 days (p=0.031), but this became non-significant soon after stopping the treatment and until the end of the study (median survival ActD 84.5 days vs vehicle 99 days) (Supplementary Figure S6B). Notably, at collection, ActD-treated mice exhibited milder AML-related pathological findings, including significantly smaller spleens, lower white blood cell and higher platelet counts (Figures 4F-4H). The anti-leukemic effect of ActD was also confirmed by the significant reduction of circulating human CD45+ AML cells in blood (Figure 4I), as well as trends towards lower levels in the bone marrow and spleen (Supplementary Figure S6C-S6D). Overall, these data show that single-agent ActD has anti-leukemic activity *in vivo* against human *NPM1*-mutant AML. Nonetheless, further studies will be needed to assess the selectivity of this treatment for NPM1c+ versus NPM1wt AML patients.

ActD potentiates the effects of Venetoclax against pre-leukemic and leukemic NPM1c+ cells

Since Venetoclax has become the standard of care for the older/unfit AML patients and is particularly effective against *NPM1*-mutant AML^{42,43}, we next wanted to examine if the ActD-Venetoclax combination could synergistically suppress the growth of NPM1c+ hematopoietic cells. We found that doses of ActD or Venetoclax that had mild effects on cell proliferation in isolation, significantly inhibited the growth of pre-leukemic *Npm1*^{cA/+} hematopoietic progenitors in liquid culture when combined (Figure 5A). Moreover, the combination of ActD and Venetoclax synergistically reduced the number of total CFU colonies in semi-solid media, at doses that had minimal anti-clonogenic effect when each drug was used in isolation (Figure 5B-5C).

In a similar fashion, ActD treatment synergistically enhanced the anti-leukemic effects of Venetoclax in murine $Npm1^{cA/+}$; $Flt3^{ITD/+}$ AML cells (Figure 4D). In the same model, high ZIP synergistic scores were obtained in MTS proliferation assays when Venetoclax was combined with low concentrations of ActD (Figure 5E, Supplementary Figure S7A).

Low-dose ActD treatment re-sensitizes resistant NPM1-mutant AML cells to Venetoclax

NPM1c-mutant OCI-AML3 cells carry biallelic loss-of-function *BAX* mutations and are resistant to Venetoclax (Supplementary Figure S7B-S7C). We pre-treated OCI-AML3 cells for 24 hours with low-dose ActD (0.5 nM), a concentration that did not affect cell viability (Supplementary Figure S7D). We then removed ActD and exposed the pre-treated cells to a range of doses of Venetoclax (Figure 5F). We found that ActD pre-treated OCI-AML3 were significantly more sensitive to Venetoclax compared to DMSO pre-treated cells, with a dramatic 5-fold reduction in IC50 (Figure 5G, Supplementary Figure S7E). In addition, Annexin V staining showed a significant increase in apoptosis induction in *NPM1*-mutant cells following combination treatment with low-dose ActD and Venetoclax (Supplementary Figure S7F).

To test if this observation held true for acquired Venetoclax resistance outside immortalized cells lines, we turned to our *Sleeping Beauty* transposon-driven NPM1c+ AML model²⁰. In brief, we exposed murine NPM1c+ AML cells harboring active (jumping) transposons to gradually increasing doses of Venetoclax, until they developed resistance. The derivative resistant AML cells displayed a 4-7x higher IC50 value for Venetoclax compared to the parental cells. However, as with the OCI-AML3 cells, pre-treatment with low concentration of ActD restored their sensitivity to Venetoclax in a dose-dependent manner (Figure 5H-5J, Supplementary Figure S7G-S7H).

NPM1c+ AML cells are preferentially sensitive to inhibition of the 40S maturation pathway

Ribosome biogenesis is a highly orchestrated process involving more than 200 different factors ⁷. ActD targets the first step in the process, namely transcription of the polycistronic 47S pre-rRNA precursor, but in higher concentrations can have pleiotropic effects and associated toxicities³⁹. Thus, we next wanted to explore whether ribosome biosynthesis could be targeted in NPM1c+ AML cells in alternative ways, by inhibiting specific ribosome-related factors.

To investigate this, we started by examining the DepMap database which contains CRIPSR knock-out data for hundreds of different cancer cell lines^{24,25}. We isolated the top 500 preferentially essential genes for OCI-AML3 (the only NPM1c+ cell line in the database), whose knock-out is more detrimental to this cell line versus other cancer cell lines. From this list, we selected all genes with a known role in ribosome biogenesis, including ribosomal components and factors involved in rRNA transcription, modification, assembly and

321 maturation (Figure 6A). Candidates recovered in the list included NPM1 itself, the rDNA 322 transcription factor UBTF, NOP56, which is a core component of box C/D small nucleolar ribonucleoprotein particles, and RPS6KA1, a member of the RSK family of kinases that is 323 involved in the phosphorylation of RPS6 and is druggable 44,45 (Supplementary Figure S8A-324 S8F). 325 326 Notably, among the list of preferentially essential genes for OCI-AML3 cells, we found an 327 enrichment for factors that are involved in related steps of the 40S ribosome maturation 328 pathway, including the ribosome assembly factors BYSL, TSR1 and TSR3. BYSL and TSR1 bind early 40S precursors in the nucleoplasm and are exported bound to the pre-40S subunit to 329 the cytoplasm, where TSR3 is then recruited for the final stages of maturation⁷. Loss of any of 330 331 these three factors had a strong, preferential anti-leukemic effect against OCI-AML3 cells, 332 compared to a panel of 37 different AML cell lines (Figure 6B-6D, Supplementary Figure S9A). 333 TSR3 is an aminocarboxypropyl (acp) transferase responsible for the hyper-modification of 334 the 18S rRNA during late 40S maturation steps in the eukaryotic cytoplasm. Unlike BYSL and TSR1 which are common essential genes^{24,25}, TSR3 is not broadly essential for cell 335 survival^{46,47}, making it an attractive therapeutic target. Notably, an independent CRISPR 336 337 knock-out screen also identified TSR3 as a specific vulnerability of OCI-AML3 cells, but not of the other 4 different AML cell lines tested (OCI-AML2, MOLM-13, HL-60 and MV-4-11)²³ 338 (Figure 6E). We decided to focus on TSR3 for validation studies for the following reasons: i) 339 specificity against NPM1c+ AML, ii) cross-validation in two independent CRISPR screens ^{23–25}, 340 iii) participation in the 40S subunit maturation, disruption of which is particularly detrimental 341 for NPM1c+ cells, iv) non-essential function in normal cells ^{46,47}, and v) potentially druggable 342 profile ⁴⁷. We confirmed that TSR3 knock-out inhibits the growth of OCI-AML3 cells (Figure 343 344 6F) but has little or no effect on the proliferation of wild-type NPM1 cell lines (Supplementary Figure S9B). In addition, *Tsr3* targeting reduced the proliferation of murine *Npm1*^{cA/+}; *Flt3*^{ITD/+} 345 leukemic cells (Figure 6G), but not of murine AML cells driven by Flt3^{ITD/+} and oncogenic MLL 346

Upregulation of p53 targets and induction of apoptosis in TSR3-depleted NPM1c+ AML cells

the non-leukemic murine hematopoietic progenitor line 32D (Figure 6H).

gene fusions (Supplementary Figure S9C). Finally, Tsr3 knock-out did not affect the growth of

347

348

349

Next, we wanted to investigate the effects of *TSR3* knock-out on NPM1c+ AML cells. RNA-seq analysis revealed the upregulation of many direct p53 target genes, including *CYFIP2*, *CDKN1A* and *PHLDA3*, shortly after *TSR3* depletion (Figure 7A, Supplementary Table S7). We performed GSEA analysis of RNA-seq from *TSR3*-depleted OCI-AML3 cells and found an enrichment for genes involved in apoptosis and a depletion of E2F targets and G2M checkpoint genes (Supplementary Figure S10A-S10C). Conversely, no apoptosis or cell cycle-related gene sets were significantly altered in *TSR3*-depleted OCI-AML2 cells (NPM1wt) at the same timepoint (Supplementary Figure S10D-S10F).

Reflecting these findings, *TSR3* knock-out increased apoptosis in OCI-AML3 cells and in murine *Npm1*^{cA/+}; *Flt3*^{ITD/+} leukemia cells (Figure 7B-7D, Supplementary Figure S10G-S10I), while also affecting cell cycle distribution (Figure 7E, Supplementary Figure S10J). In contrast, we did not observe any significant alterations in apoptosis or the cell cycle distribution upon *TSR3* knock-out in OCI-AML2 cells (Supplementary Figure S10K-S10M).

TSR3 depletion re-sensitizes resistant NPM1c+ AML cells to Venetoclax

Finally, we wanted to investigate whether *TSR3* depletion could restore Venetoclax sensitivity of resistant NPM1c+ leukemia cells, as seen with low-dose ActD treatment. For this, we knocked-out *TSR3* in OCI-AML3 cells and re-assessed response to Venetoclax (Figure 7F). Strikingly, we observed that upon *TSR3* depletion, OCI-AML3 cells responded to concentrations as low as 50 nM, whereas control gRNA-transduced cells required 100-200 times higher concentrations to display a similar effect (Figure 7G, Supplementary Figure S11A-S11B). Overall, IC50 was 4.5-fold lower in *TSR3*-depleted compared to control OCI-AML3 cells (Figure 7H, Supplementary Figure S11C).

Next, we mixed BFP-expressing control gRNA and *TSR3* gRNA-transduced OCI-AML3 cells with non-transduced cells and treated with increasing Venetoclax concentrations for a course of 5 days, while also monitoring the gRNA abundance using flow cytometry (Figure 7I). As expected, control gRNA-transduced cells showed no decreased survival in the examined concentrations. In contrast, *gTSR3*-transduced cells showed decreased survival that was additionally reduced upon Venetoclax treatment, further demonstrating the selective sensitivity of the *TSR3*-depleted cell population (Figure 7J, Supplementary Figure S11D-S11G).

Discussion

NPM1c mutations are found in 30% of all AML cases¹³. Yet, despite some recent advances in understanding their molecular consequences^{48,49}, current therapeutic outcomes remain suboptimal, highlighting the need for new effective treatments¹⁸. In this study we identified *NPM1c*-induced proteomic changes and investigated their therapeutic potential. The use of a faithful conditional knock-in mouse model allowed us to study the proteomic effects of *NPM1c* mutations in isolation, by overcoming the confounding effects of different comutations¹⁹ or other sources of biological variation including potential *in vitro* adaptive changes in transformed cell lines. This enabled us to establish a direct connection between the mutated NPM1c protein and observed phenotypes.

Our findings revealed that levels of many proteins involved in ribosome biogenesis are significantly reduced in NPM1c+ cells, without significant changes in expression of their cognate mRNAs (RNA-seq), in keeping with altered post-transcriptional regulation. This downregulation could be either directly or indirectly triggered by the reduced levels of wild-type NPM1 in mutant cells, although the precise mechanisms involved require further investigation. Potential scenarios include: i) the interaction of wild-type NPM1 with rRNA and ribosome biogenesis factors may stabilize them, with loss of this interaction in the mutant cells leading to protein degradation ii) NPM1 haploinsufficiency may alter the availability of its chaperone partners or disrupt the structural organization of the nucleolus^{9,10}, impacting interactions, levels and stability of ribosome biogenesis factors. Interestingly, the altered nucleolar structure was recently shown to be detectable by holotomography⁵⁰. Based on the observed depletion of ribosome biogenesis factors, we hypothesized that targeting nucleolar homeostasis may selectively affect NPM1c+ cells. Indeed, *NPM1*-mutant cells were selectively more sensitive to multiple RNA pol I inhibitors (ActD, CX-5461 and BMH-21) but displayed no differential response to translation inhibitors like cycloheximide.

Importantly, reduced ribosomal factor levels are also evident after leukemia development, providing a rationale for re-examining the concept of targeting ribosome biogenesis in NPM1c+ AML, as first suggested³² and tested³³ by Falini and colleagues. More recently, Gionfriddo et al. showed that ActD could induce complete remission in relapsed/refractory *NPM1*-mutant AML patients, with evidence that the treatment initiated a nucleolar stress

response³⁴. Interestingly, Wu et al. discovered an additional effect of ActD in mitochondria 412 which contributed to its anti-leukemic effects⁵¹. 413 414 In the second part of this study, we explored whether specific ribosome biogenesis factors can be targeted in NPM1-mutant leukemic cells. Using DepMap^{24,25} and another independent 415 genome-wide AML CRISPR screen²³, we identified *TSR3*, a gene whose knock-out 416 preferentially reduced the proliferation of NPM1c+ AML cells. TSR3 acts at the late 417 cytoplasmic stages of the 40S ribosome maturation and is responsible for introducing the N1-418 methyl-N3-aminocarboxypropylpseudouridine (m¹acp³Ψ) mark on 18S rRNA⁴⁷. Interestingly, 419 loss of the $m^{1}acp^{3}\Psi$ is a common event in cancer⁴⁶, though it is unclear if this loss confers a 420 421 growth advantage or is simply a by-product of the high ribosome production rates in cancer 422 cells. 423 Currently, the mechanism underlying the dependency of NPM1c+ AML on TSR3 is poorly 424 understood, and it remains uncertain if it relates to its enzymatic activity. The significantly 425 reduced levels of the ribosome factors KRI1 and its interactor KRR1, both of which are acting upstream of TSR3 in 40S maturation⁷, could provide a potential link to explain this 426 vulnerability. In this model, TSR3 knock-out, like RNA pol I inhibition, could be exacerbating an 427 428 already impaired ribosome biogenesis process in NPM1c+ AML, lowering the threshold for 429 p53 activation and leading to apoptosis. Notably, both low-dose ActD treatments and TSR3 knock-out synergized with Venetoclax and 430 431 displayed the ability to induce at least partial re-sensitization in NPM1-mutant, Venetoclax-432 resistant AML models. Previous studies have shown that nucleolar stress, such as that caused by RNA pol I inhibition, leads to the diffusion of ribosomal proteins into the nucleoplasm, 433 where they bind and sequester MDM2, resulting in p53 stabilization and upregulation of key 434 apoptotic genes^{36,52–54}. In addition, induction of p53-driven apoptosis was demonstrated in 435 ActD-treated NPM1-mutant AML cells³⁴. In line with these findings, our RNA-seq analysis of 436 437 TSR3-depleted NPM1c+ cells revealed the upregulation of direct p53 targets, including 438 CDKN1A (p21), and an enrichment for genes involved in apoptosis. Importantly, p53 and the apoptotic response network have a central role in controlling sensitivity to Venetoclax^{55,56}. 439

Taken together, these data suggest that activation of p53 and its targets by ActD or TSR3

knock-out works synergistically with BCL-2 inhibition (Venetoclax) to promote apoptosis in

440

441

442

NPM1-mutant AML cells.

Overall, our findings lead us to propose that acquisition of *NPM1c* and the accompanying loss of one wild-type *NPM1* allele result in the post-transcriptional depletion of multiple players involved in ribosome biogenesis, a consequence that can be exploited therapeutically to

target NPM1-mutant AML cells (Supplementary Figure S12).

447

446

448 Acknowledgements

- 449 This work was funded by grants from Cancer Research UK (C22324/A24482) and AstraZeneca 450 (G113590). G.S.V. is supported by a Cancer Research UK Senior Cancer Fellowship 451 (C22324/A23015) and work in his laboratory is also funded by the European Research 452 Council, Leukemia and Lymphoma Society, Rising Tide Foundation for Clinical Cancer 453 Research, Kay Kendall Leukaemia Fund, Blood Cancer UK and Wellcome Trust. A.D. is 454 supported by Cancer Research UK (C22324/A24482) and AstraZeneca (G113590). K.T., E.Y. and M.E. are supported by Wellcome Trust (grants RG94424, RG83195, RG106133 and 455 456 RG127005) and UKRI Medical Research Council (grant RG83195). K.T. and M.E. are supported 457 by Leukaemia UK (grants 2020/JGF/004 and 2022/FuF/001). E.Y. is supported by a Leukaemia 458 UK John Goldman Fellowship (2024/JGF/009). Work in the A.J.W. lab is supported by Cancer 459 Research UK (DRCNPG-Jun24/100002), the UK Medical Research Council (MR/T012412/1), 460 the European Cooperation in Science and Technology (COST) Action Translacore (CA21154), 461 Blood Cancer UK (21002), the Rosetrees Trust (PGL22/100032), Isaac Newton Trust 462 (G125517) and Addenbrookes Charitable Trust (900426). J-E.S. was supported by the 463 Programme "Investissement d'Avenir" PSPC (IMODI) and the Laboratoire d'Excellence Toulouse Cancer (TOUCAN; contract ANR11-LABEX). A.S was a fellow from the European 464 465 Regional Development Fund through the Interreg V-A Spain-France-Andorra (POCTEFA) 466 program, project PROTEOblood (EFA360/19; J-E.S).
- We would like to thank the Cancer Research UK Cambridge Institute Proteomics team, the Cambridge BRC Phenotyping Hub, the Anne McLaren Biomedical Research Facility (especially Charlotte Townend) and the Wellcome-MRC Cambridge Stem Cell Institute Genomics facility and Imaging facility (especially James Boyd) for providing expert technical assistance and support for our research project.

472

473

474

475

476

477

478

479

480

481

482

483

484

Authorship Contributions

G.S.V. conceived and supervised the study. G.S.V. and A.D. designed the experimental plan. A.D. carried out the majority of experiments with help from R.W. M.G. contributed to experimental design and provided scientific expertise. The *in vivo* PDX experiment was performed with help from G.G. (study design, animal procedures, imaging), R.A. (animal procedures, animal collection) and G.S.V. (intravenous injections). M.E. contributed to immunofluorescence imaging and animal collection and processing. M.Gu performed bioinformatic analysis and data deposition for the RNA-seq experiments. Primary AML characterization, sample collection and PDX generation were carried out by C.R. (clinician), V.D.M. (biobanking), F.V. (diagnosis), A.S. (PDX generation), B.V. (passaging and introduction of luciferase reporter) and I.J. and J.E.S. (supervision). E.K.P., A.S. and C.D.S. performed, analyzed and provided scientific expertise for the pre-leukemic TMT proteomics experiment.

- 485 E.Y., M.D., X.L., J.R and J.R. contributed to animal collection and processing. C.H. performed
- 486 polysome profiling. I.J., J.E.S, K.T, B.J.P.H, A.J.W and O.T. provided scientific expertise. G.S.V.
- and A.D. prepared the manuscript with help from all authors.

488 489

Conflict of Interest Disclosures

- 490 G.S.V. is a consultant to STRM.BIO and holds a research grant from AstraZeneca (G113590)
- that funded part of the research presented here. K.T. has received stock options and research
- 492 funding from Storm Therapeutics Ltd. O.T is an AstraZeneca employee and shareholder. All
- 493 other authors declare no competing financial interests.

494

References

496

- 497 1. Yu Y, Leonard B. Maggi Jr, Brady SN, et al. Nucleophosmin Is Essential for Ribosomal Protein L5 Nuclear Export. *Mol Cell Biol.* 2006;26(10):3798.
- 2. Colombo E, Marine JC, Danovi D, Falini B, Pelicci PG. Nucleophosmin regulates the stability and transcriptional activity of p53. *Nat Cell Biol*. 2002;4(7):529–533.
- Itahana K, Bhat KP, Jin A, et al. Tumor Suppressor ARF Degrades B23, a Nucleolar
 Protein Involved in Ribosome Biogenesis and Cell Proliferation. *Mol Cell*.
 2003;12:1151–1164.
- Swaminathan V, Kishore AH, Febitha KK, Kundu TK. Human Histone Chaperone
 Nucleophosmin Enhances Acetylation-Dependent Chromatin Transcription. *Molecular and Cellular Biology* . 2005;25(17):7534–7545.
- 507 5. Lee SY, Park J-H, Kim S, et al. A proteomics approach for the identification of nucleophosmin and heterogeneous nuclear ribonucleoprotein C1/C2 as chromatin-binding proteins in response to DNA double-strand breaks. *Biochem. J.* 2005;388:7–15.
- 511 6. Okuda M. The role of nucleophosmin in centrosome duplication. *Oncogene*. 2002;21:6170–6174.
- 513 7. Dörner K, Ruggeri C, Zemp I, Kutay U. Ribosome biogenesis factors—from names to functions. *EMBO J.* 2023;42(7):e112699.
- Feric M, Vaidya N, Harmon TS, et al. Coexisting liquid phases underlie nucleolar subcompartments. *Cell.* 2016;165(7):1686.
- 517 9. Mitrea DM, Cika JA, Guy CS, et al. Nucleophosmin integrates within the nucleolus via multi-modal interactions with proteins displaying R-rich linear motifs and rRNA. *Elife*. 2016;5:e13571.
- 520 10. Mitrea DM, Cika JA, Stanley CB, et al. Self-interaction of NPM1 modulates multiple mechanisms of liquid-liquid phase separation. *Nat Commun.* 2018;9(1):842.
- 522 11. Nachmani D, Bothmer AH, Grisendi S, et al. Germline NPM1 mutations lead to 523 altered rRNA 2'-O-methylation and cause dyskeratosis congenita. *Nat Genet*. 524 2019;51(10):1518–1529.
- 525 12. Falini B, Mecucci C, Tiacci E, et al. Cytoplasmic nucleophosmin in acute 526 myelogenous leukemia with a normal karyotype. *N Engl J Med*. 2005;352(3):254–266.
- 527 13. Papaemmanuil E, Gerstung M, Bullinger L, et al. Genomic Classification and Prognosis in Acute Myeloid Leukemia. *New England Journal of Medicine*.
- 529 2016;374(23):2209–2221.

- 530 14. Falini B, Bolli N, Liso A, et al. Altered nucleophosmin transport in acute myeloid leukaemia with mutated NPM1: molecular basis and clinical implications. *Leukemia* 2009 23:10. 2009;23(10):1731–1743.
- 533 15. Döhner K, Thiede C, Jahn N, et al. Impact of NPM1/FLT3-ITD genotypes defined by the 2017 European LeukemiaNet in patients with acute myeloid leukemia. *Blood*. 2020;135(5):371.
- 536 16. Stone RM, Mandrekar SJ, Sanford BL, et al. Midostaurin plus Chemotherapy for Acute Myeloid Leukemia with a FLT3 Mutation. *N Engl J Med*. 2017;377(5):454.
- 538 17. Short NJ, Konopleva M, Kadia TM, et al. Advances in the treatment of acute myeloid leukemia: New drugs and new challenges. *Cancer Discov.* 2020;10(4):506–525.
- 540 18. Ranieri R, Pianigiani G, Sciabolacci S, et al. Current status and future perspectives in targeted therapy of NPM1-mutated AML. *Leukemia* 2022 36:10. 2022;36(10):2351–2367.
- 543 19. Yun H, Narayan N, Vohra S, et al. Mutational synergy during leukemia induction 544 remodels chromatin accessibility, modification and 3-Dimensional DNA topology to 545 alter gene expression. *Nat Genet*. 2021;53(10):1443.
- 546 20. Vassiliou GS, Cooper JL, Rad R, et al. Mutant nucleophosmin and cooperating 547 pathways drive leukemia initiation and progression in mice. *Nat Genet*. 548 2011;43(5):470.
- 549 21. Dovey OM, Cooper JL, Mupo A, et al. Molecular synergy underlies the co-occurrence 550 patterns and phenotype of NPM1-mutant acute myeloid leukemia. *Blood*. 551 2017;130(17):1911–1922.
- 552 22. Kramer MH, Zhang Q, Sprung R, et al. Proteomic and phosphoproteomic landscapes of acute myeloid leukemia. *Blood*. 2022;140(13):1533–1548.
- 554 23. Konstantinos Tzelepis A, Koike-Yusa H, De Braekeleer E, et al. A CRISPR Dropout
 555 Screen Identifies Genetic Vulnerabilities and Therapeutic Targets in Acute Myeloid
 556 Leukemia. CellReports. 2016;17:1193–1205.
- 557 24. Meyers RM, Bryan JG, McFarland JM, et al. Computational correction of copy-558 number effect improves specificity of CRISPR-Cas9 essentiality screens in cancer 559 cells. *Nat Genet*. 2017;49(12):1779.
- Dempster JM, Rossen J, Kazachkova M, et al. Extracting Biological Insights from the
 Project Achilles Genome-Scale CRISPR Screens in Cancer Cell Lines. *BioRxiv*.
 2019;720243:.
- 563 26. Sasaki T, Toh-e A, Kikuchi Y. Yeast Krr1p physically and functionally interacts with a novel essential Kri1p, and both proteins are required for 40S ribosome biogenesis in the nucleolus. *Mol Cell Biol*. 2000;20:7971–7979.
- 566 27. Ge W, Wolf A, Feng T, et al. Oxygenase-catalyzed ribosome hydroxylation occurs in prokaryotes and humans. *Nat Chem Biol*. 2012;8(12):960–962.
- Wu S, Tutuncuoglu B, Yan K, et al. Diverse roles of assembly factors revealed by structures of late nuclear pre-60S ribosomes. *Nature*. 2016;534(7605):133–137.
- 570 29. Hua Y, Song J, Peng C, et al. Advances in the Relationship Between Regulator of Ribosome Synthesis 1 (RRS1) and Diseases. *Front Cell Dev Biol.* 2021;9:620925.
- O'Leary MN, Schreiber KH, Zhang Y, et al. The Ribosomal Protein Rpl22 Controls
 Ribosome Composition by Directly Repressing Expression of Its Own Paralog,
 Rpl2211. *PLoS Genet*. 2013;9(8):e1003708.
- Sasaki T, Toh-e A, Kikuchi Y. Yeast Krr1p Physically and Functionally Interacts with
 a Novel Essential Kri1p, and Both Proteins Are Required for 40S Ribosome
 Biogenesis in the Nucleolus. *Mol Cell Biol*. 2000;20(21):7971.

- 578 32. Falini B, Gionfriddo I, Cecchetti F, et al. Acute myeloid leukemia with mutated nucleophosmin (NPM1): Any hope for a targeted therapy? *Blood Rev*. 2011;25(6):247–254.
- 581 33. Falini B, Brunetti L, Martelli MP. Dactinomycin in NPM1 -Mutated Acute Myeloid 582 Leukemia . *New England Journal of Medicine*. 2015;373(12):1180–1182.
- 583 34. Gionfriddo I, Brunetti L, Mezzasoma F, et al. Dactinomycin induces complete 584 remission associated with nucleolar stress response in relapsed/refractory NPM1-585 mutated AML. *Leukemia*. 2021;35(9):2552–2562.
- 586 35. Burger K, Mü hl B, Harasim T, et al. Chemotherapeutic Drugs Inhibit Ribosome 587 Biogenesis at Various Levels. *Journal of Biological Chemistry*. 2010;285(16):12416– 588 12425.
- 589 36. Carmen Lafita-Navarro M, Conacci-Sorrell M. Nucleolar stress: From development to cancer. *Semin Cell Dev Biol.* 2023;136:64–74.
- 591 37. Potapova TA, Unruh JR, Conkright-Fincham J, et al. Distinct states of nucleolar stress induced by anticancer drugs. *Elife*. 2023;12:RP88799.
- 593 38. Yat-Ming Yung B, Chang F-J, Meei-Shuu Bor A, Siew-Teh Lee E. Schedule-594 dependent effects of two consecutive, divided, low doses of actinomycin D on 595 translocation of protein B23, inhibition of cell growth and RNA synthesis in hela cells. 596 *Int. J. Cancer.* 1992;52:317–322.
- 597 39. Ferreira R, Schneekloth JS, Panov KI, Hannan KM, Hannan RD. Targeting the RNA 598 Polymerase I Transcription for Cancer Therapy Comes of Age. *Cells*. 2020;9(2):266.
- 599 40. Peltonen K, Colis L, Liu H, et al. A targeting modality for destruction of RNA polymerase I that possesses anticancer activity. *Cancer Cell*. 2014;25(1):77–90.
- Drygin D, Lin A, Bliesath J, et al. Targeting RNA polymerase I with an oral small
 molecule CX-5461 inhibits ribosomal RNA synthesis and solid tumor growth. *Cancer Res.* 2011;71(4):1418–1430.
- 604 42. Dinardo CD, Pratz K, Pullarkat V, et al. Venetoclax combined with decitabine or azacitidine in treatment-naive, elderly patients with acute myeloid leukemia. *Blood*. 2019;133(1):7–17.
- Lachowiez CA, Loghavi S, Kadia TM, et al. Outcomes of older patients with NPM1-mutated AML: Current treatments and the promise of venetoclax-based regimens.
 Blood Adv. 2020;4(7):1311–1320.
- Weidenauer K, Schmidt C, Rohde C, et al. The ribosomal protein S6 kinase alpha-1
 (RPS6KA1) induces resistance to venetoclax/azacitidine in acute myeloid leukemia.
 Leukemia. 2023;37(8):1611–1625.
- Sapkota GP, Cummings L, Newell FS, et al. BI-D1870 is a specific inhibitor of the
 p90 RSK (ribosomal S6 kinase) isoforms in vitro and in vivo. *Biochemical Journal*.
 2007;401(1):29–38.
- 46. Babaian A, Rothe K, Girodat D, et al. Loss of m 1 acp 3 J Ribosomal RNA
 Modification Is a Major Feature of Cancer. *Cell Rep.* 2020;31(5):107611.
- Meyer B, Wurm JP, Sharma S, et al. Ribosome biogenesis factor Tsr3 is the
 aminocarboxypropyl transferase responsible for 18S rRNA hypermodification in yeast
 and humans. *Nucleic Acids Res.* 2016;44(9):4304–4316.
- 48. Uckelmann HJ, Haarer EL, Takeda R, et al. Mutant NPM1 directly regulates
 oncogenic transcription in acute myeloid leukemia. *Cancer Discov*. 2023;13(3):746–
 765.
- 49. Wang XQD, Fan D, Han Q, et al. Mutant NPM1 Hijacks Transcriptional Hubs to
 625 Maintain Pathogenic Gene Programs in Acute Myeloid Leukemia. *Cancer Discov*.
 626 2023;13(3):724–745.

- 627 50. Kim H, Kim G, Park HJ, et al. Integrating holotomography and deep learning for rapid 628 detection of NPM1 mutations in AML. Sci Rep. 2024;14(1):23780.
- 629 Wu H-C, Rérolle D, Berthier C, et al. Actinomycin D Targets NPM1c-Primed 51. 630 Mitochondria to Restore PML-Driven Senescence in AML Therapy. *Cancer Discov*. 631 2021;11(12):3198–3213.
- Lohrum MAE, Ludwig RL, Kubbutat MHG, Hanlon M, Vousden KH. Regulation of 632 52. 633 HDM2 activity by the ribosomal protein L11. Cancer Cell. 2003;3(6):577–587.
- Horn HF, Vousden KH. Cooperation between the ribosomal proteins L5 and L11 in 634 53. 635 the p53 pathway. Oncogene. 2008;27(44):5774–5784.
- 636 54. Zheng J, Lang Y, Zhang Q, et al. Structure of human MDM2 complexed with RPL11 reveals the molecular basis of p53 activation. Genes Dev. 2015;29(14):1524–1534. 637
- Nechiporuk T, Kurtz SE, Nikolova O, et al. The TP53 apoptotic network is a primary 638 55. 639 mediator of resistance to BCL2 inhibition in AML cells. Cancer Discov. 640 2019;9(7):910–925.
- Pan R, Ruvolo V, Mu H, et al. Synthetic Lethality of Combined Bcl-2 Inhibition and 641 56. p53 Activation in AML: Mechanisms and Superior Antileukemic Efficacy. Cancer 642 643 Cell. 2017;32(6):748-760.e6.

647 Figure Legends

644

645

646

648

664

665

- Figure 1. Reduced abundance of ribosomal proteins in Npm1^{cA/+} hematopoietic progenitors. 649
- (A) Workflow for global quantitative proteomic study of lineage negative (lin-) bone marrow-650 derived hematopoietic progenitors using tandem-mass tagging (TMT). Pre-leukemic Npm1^{cA/+} 651
- (n=7) vs $Npm1^{+/+}$ (n=5) murine hematopoietic progenitors were collected 8 weeks after Mx1-652
- Cre induction with polyinosinic:polycytidylic acid (plpC). (B) Volcano plot showing relative 653 protein abundances in pre-leukemic $Npm1^{cA/+}$ vs $Npm1^{+/+}$ lin- progenitors. (C-F) Relative
- 654 abundance of selected ribosome-related proteins in $Npm1^{cA/+}$ vs $Npm1^{t/+}$ lin- progenitors. (G)
- 655
- Overlap between mRNAs (RNA-seq) and proteins (LC-MS) that were significantly over- or 656 under-expressed in pre-leukemic $Npm1^{cA/+}$ vs $Npm1^{+/+}$ lin- cells. 657
- Panel (B): unpaired t-test with multiple-hypothesis-testing correction (False Discovery Rate, 658
- 659 FDR; Benjamini-Hochberg). Panels (C-F): unpaired t-test with multiple-hypothesis-testing
- 660 correction (False Discovery Rate, FDR; Benjamini-Hochberg) (*, $p \le 0.05$; **, $p \le 0.01$; ***, $p \le 0.01$;
- 0.001, ****, $p \le 0.0001$). Data represent n=7 (Npm1^{cA/+}) or n=5 (Npm1^{+/+}) biological replicates 661
- (mean \pm SD). (A) and (G) were created with Biorender. LC-MS TMT = liquid chromatography 662
- 663 mass spectrometry, tandem-mass tagging

Figure 2. Depletion of ribosome processing factors in human NPM1c+ AML.

- (A) Volcano plot of protein abundance in bone marrow samples from NPM1c+ (n=8) versus 666
- NPM1wt (n=36) human de novo AMLs²². (B-I) Relative (B-E) protein or (F-I) RNA abundance of 667
- selected ribosome-related candidates in NPM1c+ (n=8) vs NPM1wt (n=36) AML patients 668
- 669 $(mean \pm SD).$
- 670 Panel (A): unpaired t-test with multiple-hypothesis-testing correction (FDR, Benjamini-
- Hochberg method). Panels (B-I): unpaired t-test was used to calculate p values between 671

672 groups (*, $p \le 0.05$; **, $p \le 0.01$; ***, $p \le 0.001$, ****, $p \le 0.0001$). Data available in Kramer et al²².

Figure 3. Pre-leukemic Npm1^{cA/+} cells show enhanced sensitivity to RNA pol I inhibitors.

(A) Relative proliferation of pre-leukemic $Npm1^{cA/+}$ vs $Npm1^{+/+}$ lin- cells after 4 days of treatment with Actinomycin D (ActD) at the indicated doses (MTS assay). (B) Representative colony-forming unit (CFU) assays from pre-leukemic $Npm1^{cA/+}$ vs $Npm1^{+/+}$ lin- cells after 24h pre-treatment with 2.5 nM ActD. (C) Total number of colonies in CFU assays of pre-leukemic $Npm1^{cA/+}$ vs $Npm1^{+/+}$ lin-cells after 24h pre-treatment with 2.5 nM of ActD. (D) Nucleolar morphology of $Npm1^{+/+}$ (top panel) or $Npm1^{cA/+}$ (bottom panel) lin- cells after treatment with 1 nM ActD for 18h, highlighted using fluorescent staining for wild-type NPM1 (NPM1_{WT}) and nucleolin (NCL) (scale 10 μ M). (E-G) Relative proliferation of pre-leukemic $Npm1^{cA/+}$ vs $Npm1^{+/+}$ lin- cells after 4 days of treatment with (E) BMH-21, (F) CX-5461 or (G) cycloheximide at the indicated doses (MTS assay).

Panels (A), (C) and (E-G): unpaired t-test was used to calculate p values between groups (*, $p \le 0.05$; **, $p \le 0.01$; ***, $p \le 0.001$, ****, $p \le 0.0001$). Panels (A) and (E-G): absorbance values were normalized to DMSO-treated cells. Data represent 4-7 biological replicates per group (mean \pm SD). Panel (C): values represent 4 biological replicates per group. Panel (D): representative example from 1 of 2-4 biological replicates.

Figure 4. Actinomycin D reduces AML burden in a xenograft model.

(A) Schematic representation of patient-derived xenograft (PDX) experiment. Mice transplanted with 10⁶ luciferase-expressing NPM1c+AML PDX cells were treated with 0.1 mg kg⁻¹ ActD or vehicle twice weekly for 5 weeks, followed by treatment with 0.06 mg kg⁻¹ ActD or vehicle once weekly for another 3 weeks. Leukemia burden was monitored by bioluminescence imaging and quantified in tissues after animal collection. (B-D) Bioluminescence radiance on (B) day 34 (baseline), (C) day 45 and (D) day 58 in ActD vs vehicle-treated animals. (E) Bioluminescence imaging of animals treated with ActD vs vehicle at indicated timepoints. (F) Spleen weights and representative spleen pictures in ActD vs vehicle-treated animals. (G-H) Counts of (G) white blood cells and (H) platelets in ActD vs vehicle-treated animals. (I) Percentage of cells expressing human CD45 (hCD45) of total CD45 in blood in ActD vs vehicle-treated animals.

Panels (C-D) and (F-I): unpaired t-test was used to calculate p values between groups (*, $p \le 0.05$; **, $p \le 0.01$; ***, $p \le 0.001$, ****, $p \le 0.0001$). Data represent 4-6 biological replicates per group (those with available tissues upon disease presentation) (mean \pm SD). (A) was created with Biorender.

Figure 5. Actinomycin D enhances cytotoxicity and reverses resistance to Venetoclax in NPM1c+ pre-leukemic and leukemic cells.

(A) Counts of pre-leukemic $Npm1^{cA/+}$ lin- cells treated with DMSO, ActD, Venetoclax (Ven) or combination (mean \pm SD, n=3 independent experiments). (B) Representative CFU assays of pre-leukemic $Npm1^{cA/+}$ lin- cells treated with DMSO, ActD, Ven or combination. (C) Total CFU colony numbers of pre-leukemic $Npm1^{cA/+}$ lin- cells treated with DMSO, ActD, Ven or combination (n=2 biological replicates, each performed in duplicate). (D) Counts of murine $Npm1^{cA/+}$; $Flt3^{ITD/+}$ AML cells treated with DMSO, ActD, Ven or combination (mean \pm SD, n=3 independent experiments). (E) Representative synergy plot showing the interaction between

ActD and Ven in inhibiting the proliferation of murine $Npm1^{cA/+}$; $Flt3^{ITD/+}$ AML cells after 4 days of drug incubation (MTS assay) (representative example from 1 of 3 independent experiments). **(F)** OCI-AML3 cells were pre-treated with 0.5 nM ActD vs DMSO for 24 hours and then tested for sensitivity to Venetoclax. **(G)** IC50 values of DMSO or ActD pre-treated OCI-AML3 cells after 4 days of incubation with Ven at the indicated doses (MTS assay). **(H)** Outline of approach to generate Ven-resistant murine Npm1c-mutant AML cells by treatment with escalating concentrations of Ven. Ven-resistant cells were then pre-treated with ActD for 24 hours and their sensitivity to Ven was assessed using the MTS assay. **(I)** Relative proliferation of DMSO or ActD pre-treated murine NPM1c+ AML cells after 4 days incubation with Ven at the indicated doses. Absorbance values were normalized to DMSO-treated cells (mean \pm SD, data from 1 of 2 biological replicates, performed in triplicate). **(J)** IC50 values of DMSO or ActD pre-treated murine NPM1c+ AML cells after 4 days of incubation with Ven (mean \pm SD, data from 1 of 2 biological replicates, performed in triplicate).

731 Panels (A), (C-D), (G) and (J): t-test was used to calculate p values between groups (*, $p \le 0.05$; **, $p \le 0.01$; ***, $p \le 0.001$, ****, $p \le 0.0001$). (F) and (H) were created with Biorender.

Figure 6. NPM1c+ AML cells are preferentially sensitive to the inhibition of *TSR3* and related ribosome biogenesis factors.

(A) Analysis of DepMap data was used to identify the top 500 preferentially essential genes for the OCI-AML3 cell line. Of these, candidates with an established role in ribosome biogenesis are highlighted (right). The *gene_effect* represents the dependency score of each candidate for OCI-AML3 cells, where a score of 0 indicates that the gene is not essential, whereas a score of -1 corresponds to the median of all common essential genes in the database. The *mean* represents the mean gene effect across all cancer cell lines in the database. (B-D) Differential dependency of 37 AML cell lines to CRISPR knock-out of (B) *TSR1*, (C) *BYSL* or (D) *TSR3* according to DepMap. (E) Venn Diagram of gene drop-outs in a CRISPR screen with 5 AML cell lines (OCI-AML3, OCI-AML2, MOLM-13, HL-60 and MV-4-11)²³. (F-H): Relative proliferation of (F) OCI-AML3, (G) murine *Npm1*^{cA/+}; *Flt3*^{ITD/+}AML or (H) non-leukemic 32D cells upon knock-out of *TSR3* as measured by a competitive proliferation assay of gRNA-BFP positive (BFP+) transduced cells vs untransduced BFP negative (BFP-) cells over 15-18 days. BFP percentage was normalized to the day 4 reading and for (G) also to the *gControl* (mean ± SD, n=3 independent experiments).

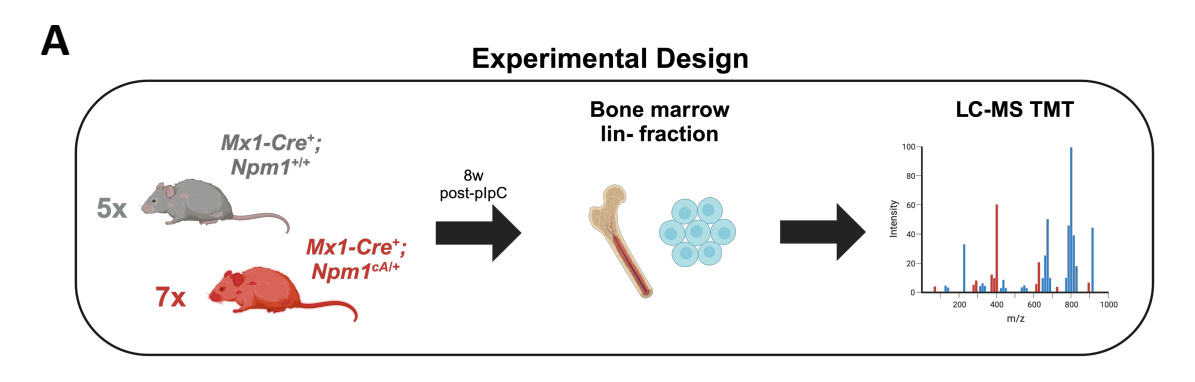
750 Panels (F-G): t-test was used to calculate p values between groups (*, $p \le 0.05$; **, $p \le 0.01$; 751 ***, $p \le 0.001$, ****, $p \le 0.0001$). Panels (A-D): CRISPR scores originate from the DepMap Public 23Q2+Score, Chronos dataset^{24,25}. (A) was created with Biorender.

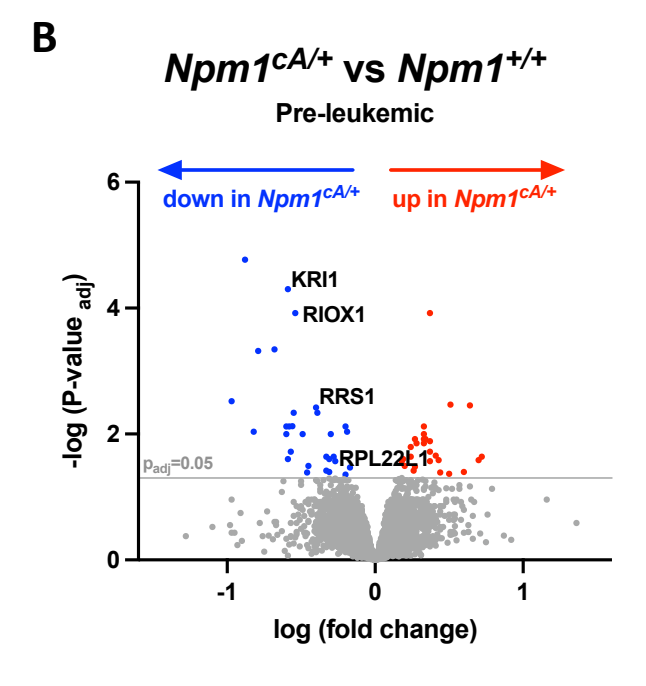
Figure 7. *TSR3* knock-out activates a p53-dependent response and re-sensitizes resistant NPM1c+ AML cells to Venetoclax.

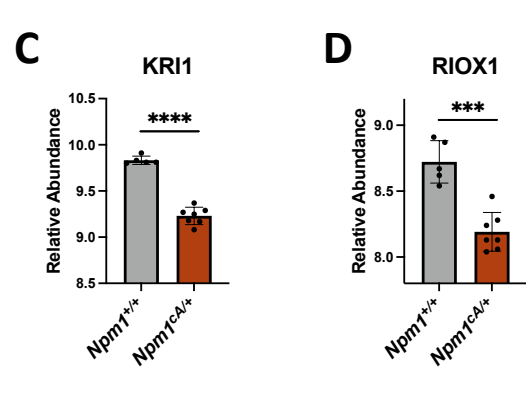
(A) Volcano plot showing differentially expressed genes in OCI-AML3 cells transduced with a *TSR3* gRNA (*gTSR3*) versus a non-targeting control gRNA (*gControl*). (B) Representative histogram plot of Annexin V staining in g*TSR3* vs *gControl*-transduced OCI-AML3 cells. (C) Annexin V staining, (D) TUNEL staining and (E) Cell cycle distribution in g*TSR3* vs *gControl*-transduced OCI-AML3 cells. (F) Schematic representation of the OCI-AML3 pre-sensitization experiment. OCI-AML3 cells were transduced with *gTSR3* or *gControl* and their response to Ven was assessed using the MTS assay. (G) Proliferation of g*TSR3* vs *gControl*-transduced OCI-AML3 cells after 4 days of incubation with Ven at the indicated doses (MTS assay). (H) IC50

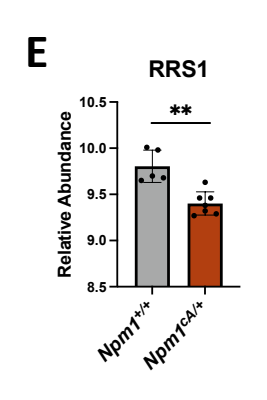
values of gTSR3 vs gControl-transduced OCI-AML3 cells after 4 days of incubation with Ven (MTS assay). (I) Schematic representation of re-sensitization experiment using OCI-AML3 cells. Cells were transduced with BFP-expressing gTSR3 or gControl and were mixed with BFP-negative untransduced cells. Next, they were exposed to Ven and the BFP+ percentage was monitored for a course of 5 days by flow cytometry. (J) Percentage of BFP+ gTSR3 or gControl-transduced cells upon treatment with Ven at the indicated doses. BFP percentage was normalized to the reading of day 1.

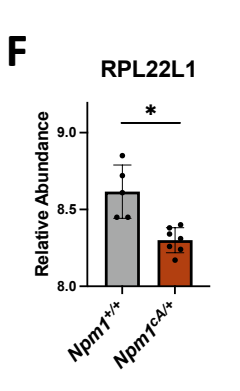
Panel (A): unpaired t-test with multiple-hypothesis-testing correction (FDR, Benjamini-Hochberg method). Panels (C-E), (G-H) and (J): t-test was used to calculate p values between groups (*, $p \le 0.05$; **, $p \le 0.01$; ***, $p \le 0.001$, ****, $p \le 0.001$). Data represent 3-6 independent experiments (mean \pm SD). Panel (G-H): absorbance values were normalized to DMSO-treated cells. Data represent 3 independent experiments (mean \pm SD). (F) and (I) were created with Biorender. MFI = Mean fluorescence intensity

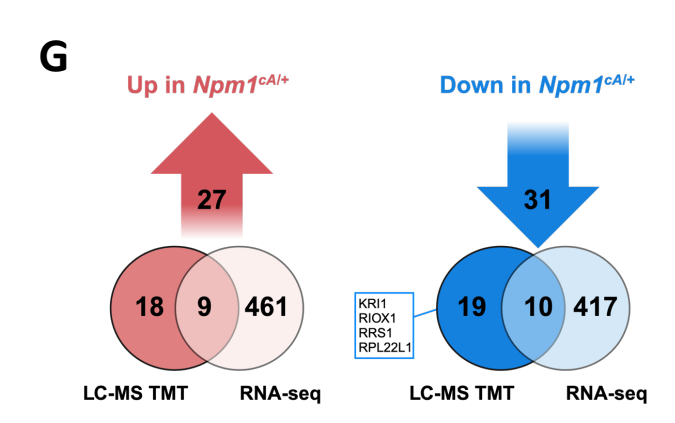


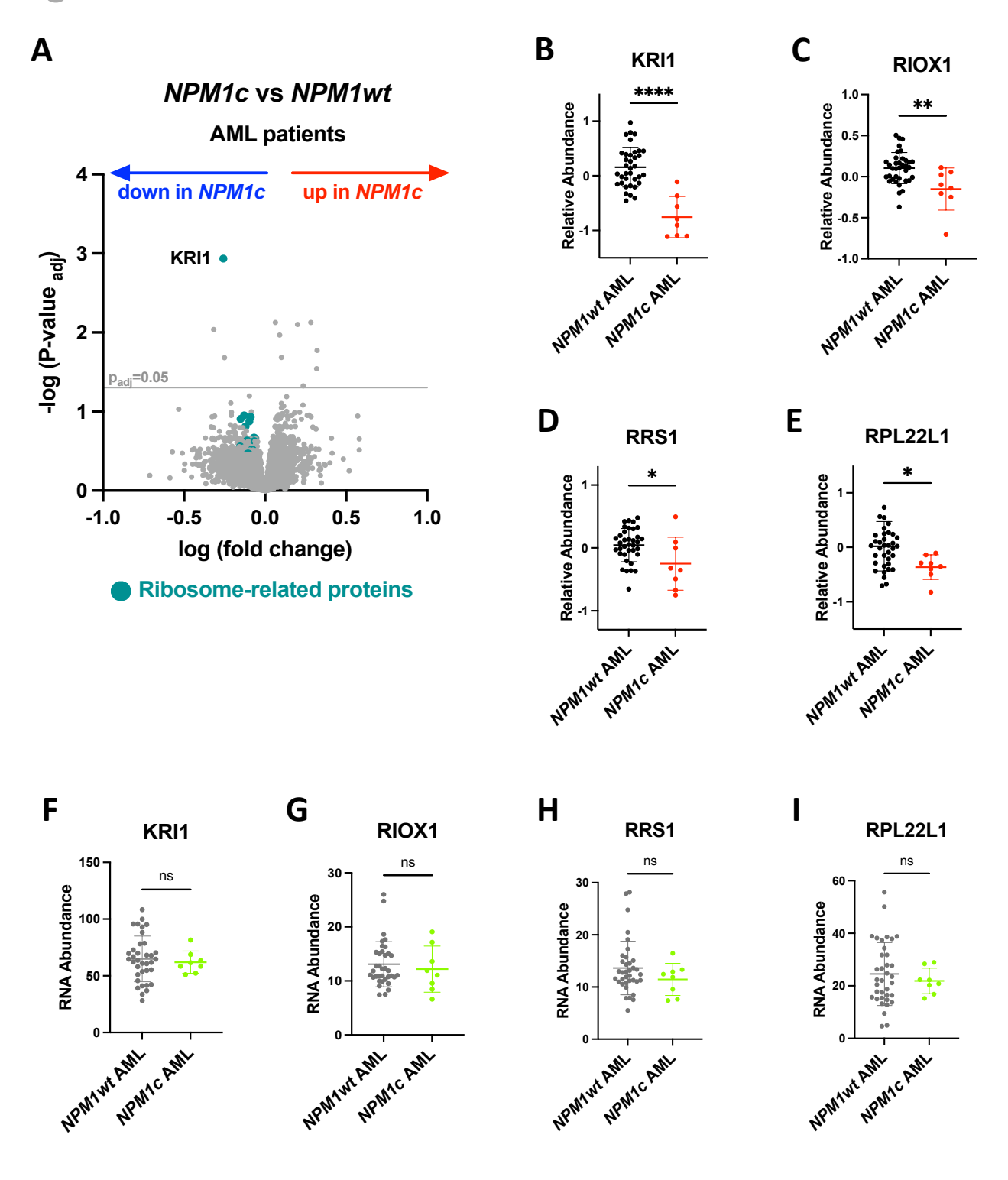


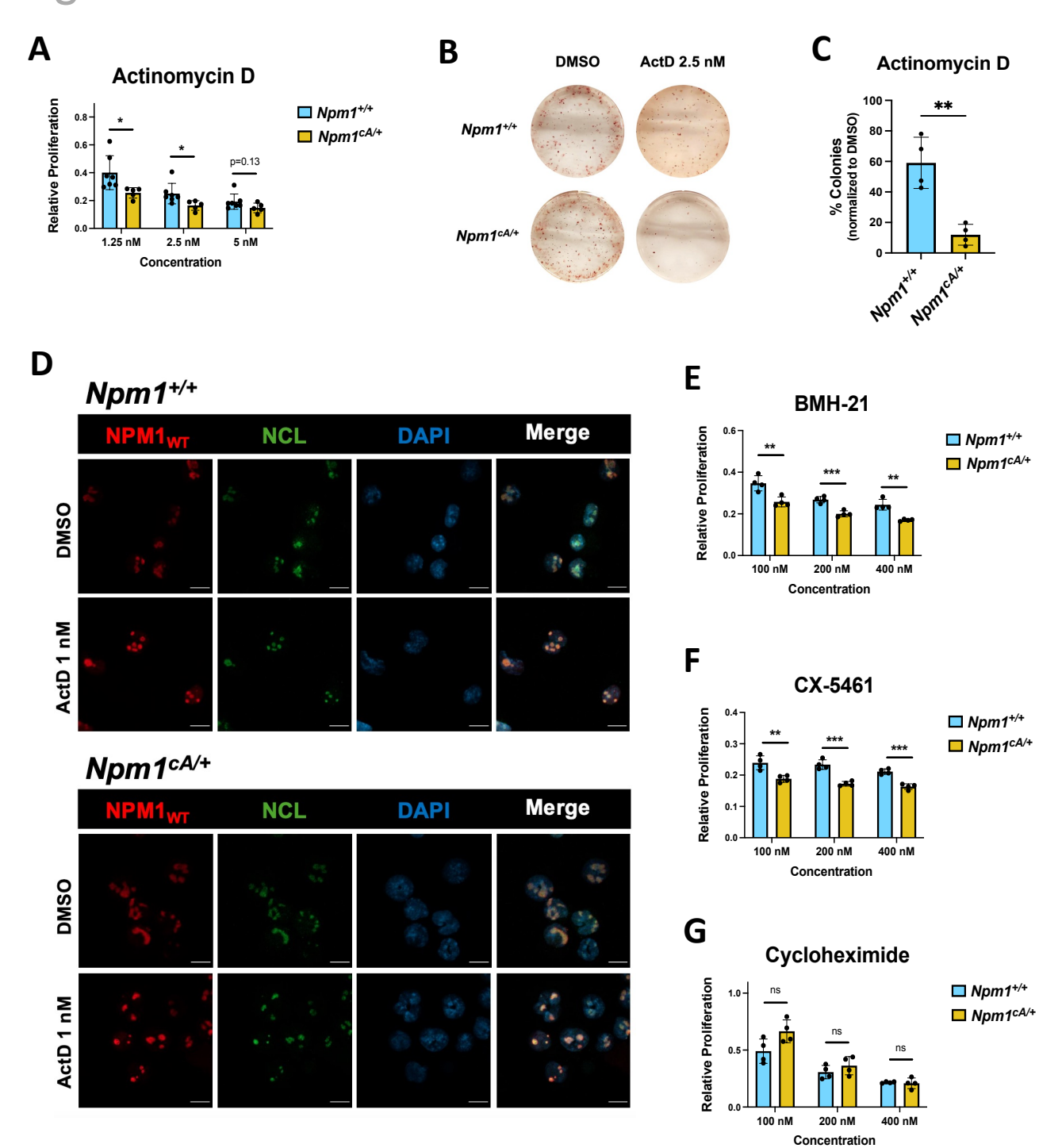


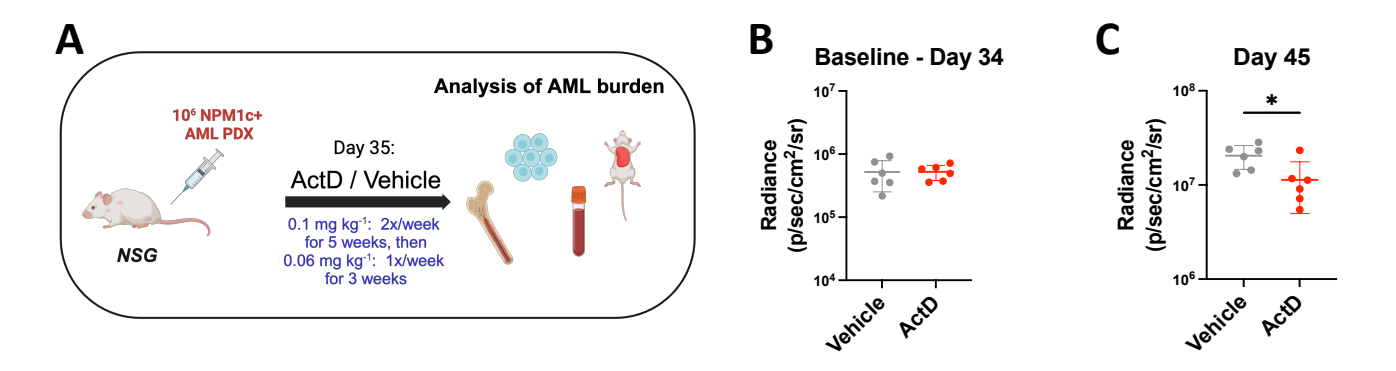


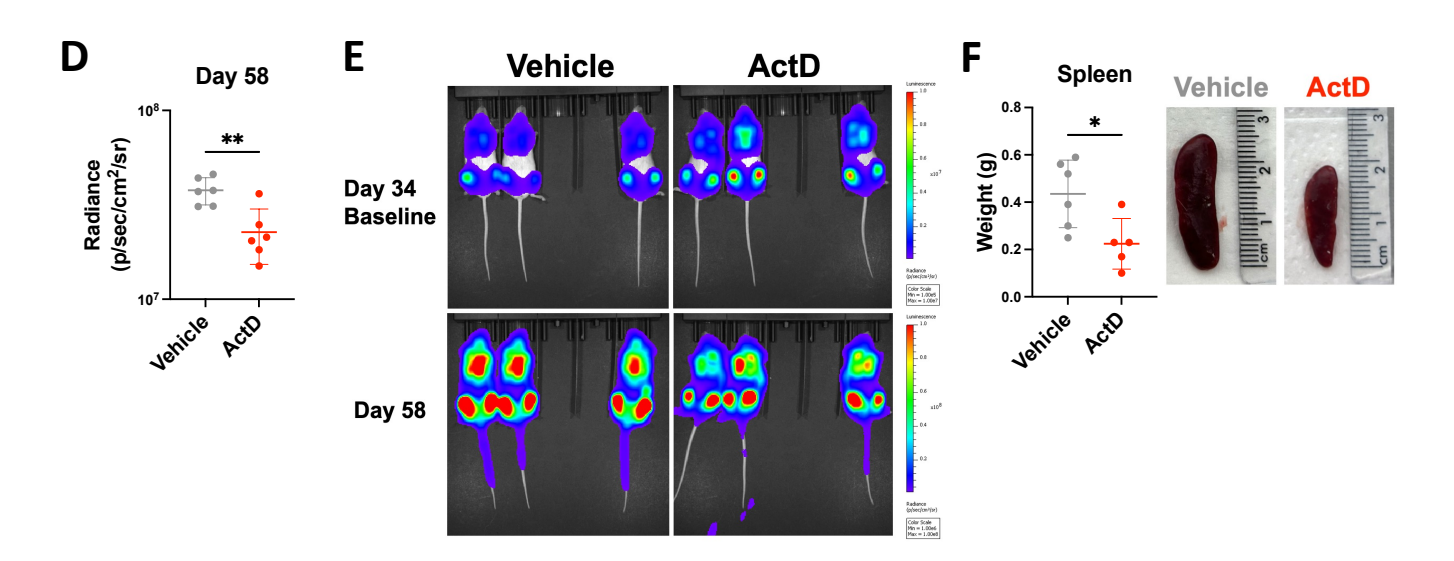


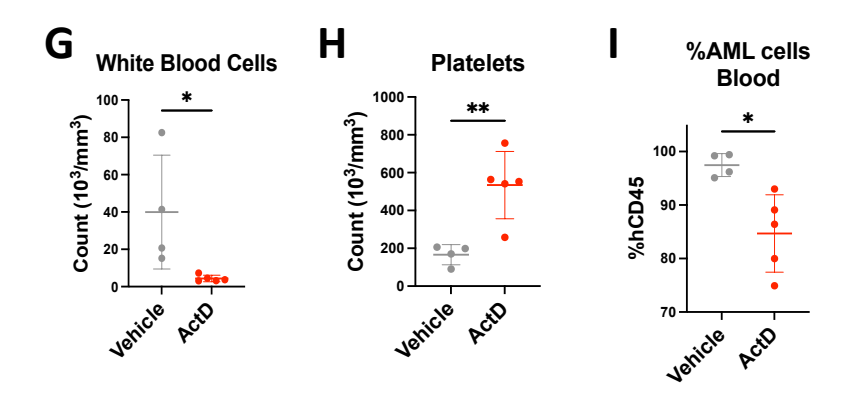






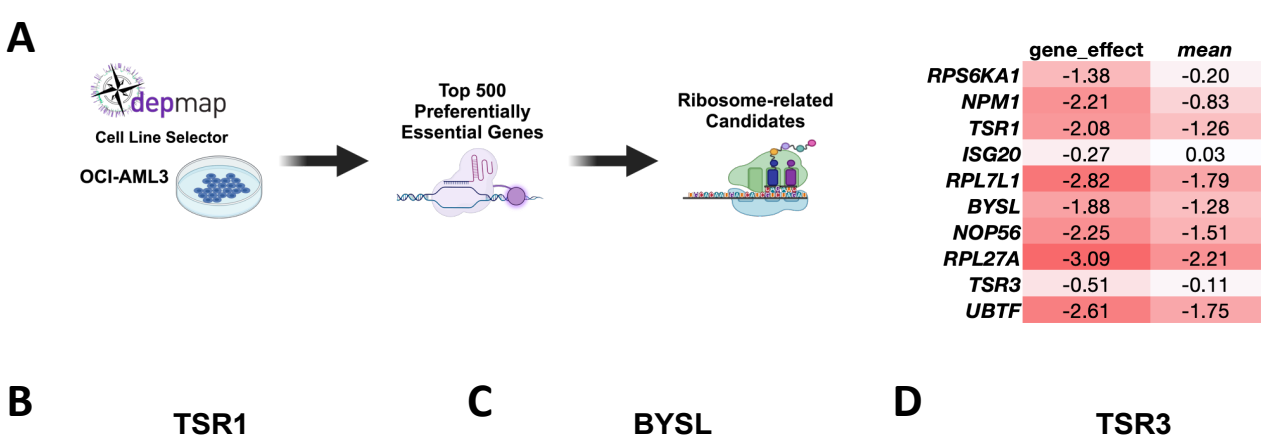


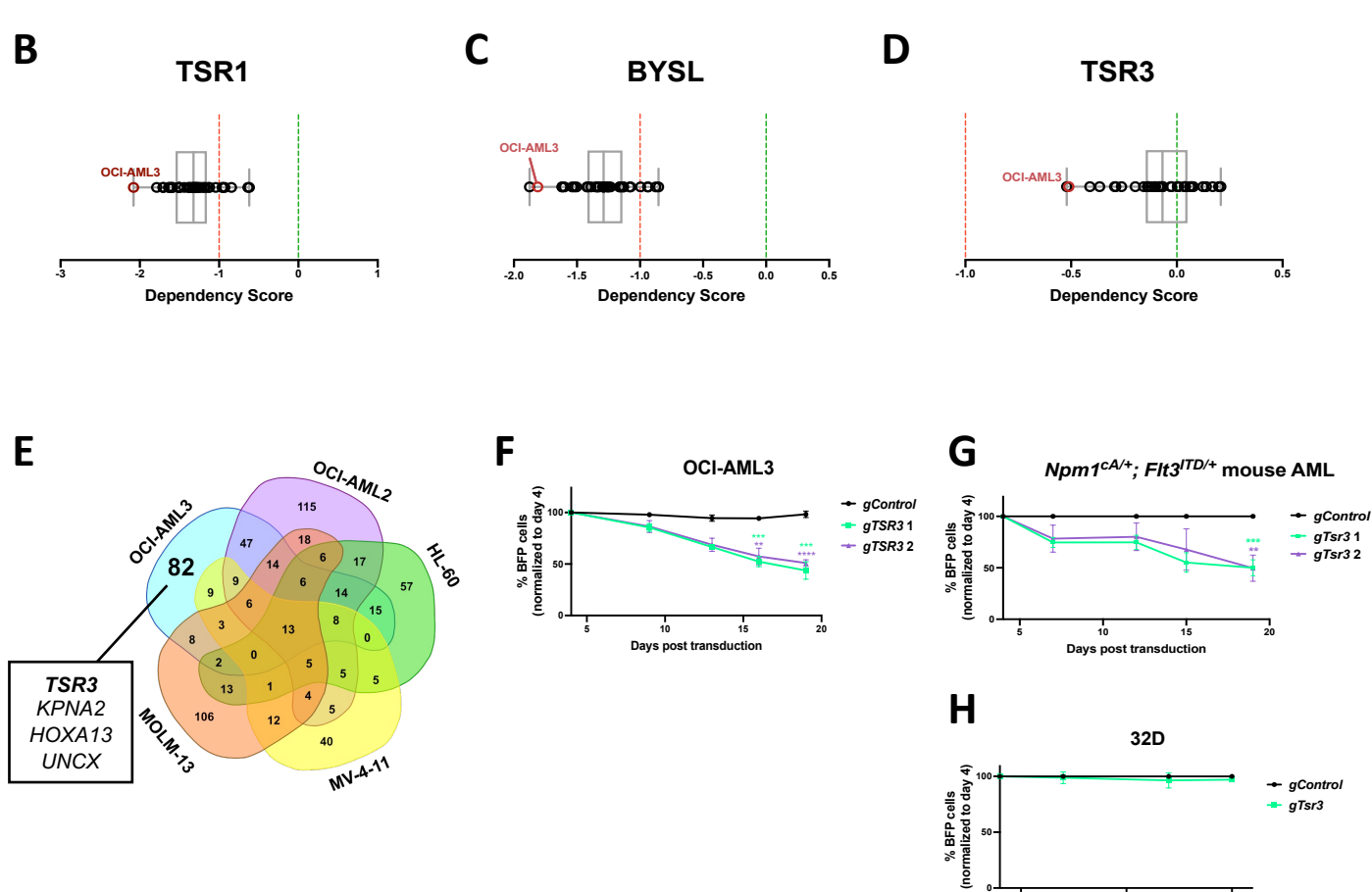




10-1

100 Venetoclax (μΜ)





Days post transduction

